Structural and optical studies of La doped, Cu co-doped ZnO nanoparticles by Co-Precipitation method

D.Anbuselvan[a] S.Anandan [b], S.Nilavazhagan[c*] , A.Santhanam[d]

a- P.G. and Research Department of Physics,Rajah Serfoji Government College, Thanjavur-5

b -P.G.and Research,Department of Physics,Thiru.Vi.Ka.Govt Arts College Thiruvarur-3

c*corresponding author - P.G.and Research Department of Physics, Rajah Serfoji Government College, Thanjavur-5

d- P.G. and Research Department of Physics,Rajah Serfoji Government College, Thanjavur-5

(affiliated to Bharathidasan university)

Abstract

$Zn_{0.96-x}La_{0.04}Cu_xO_2$ (x = 0, 0.02 & 0.04) nanoparticles have been synthesized by a co-precipitation method. The synthesized nanoparticles have been characterized by powder X-ray diffraction, energy-dispersive X-ray spectra, Scanning electron microscope, UV–Visible spectrophotometer and Fourier transform infrared spectroscopy. The XRD measurements reveal that the prepared samples   were found to be hexagonal wurtzite. The change in lattice parameters was discussed based on the secondary phase formation and presence of Cu^{2+} in LaO and ZnO_2 lattice. The variation in size and shape of the nanoparticles by Cu-doping was discussed using a scanning electron microscope. The chemical stoichiometry of Zn, Cu, La, and O was confirmed by energy-dispersive X-ray spectra. The best optical transparency observed at $Zn_{0.92}La_{0.04}Cu_{0.04}O$ nanoparticles seems to be optimal for industrial applications especially as a transparent electrode.

Keywords: XRD, Bandgab, absorbence, optical transparency,optical electrode.

1. Introduction

Semiconductor materials are the most important aspect of the ongoing research activity across the world. As the semiconductor particles are size-dependent properties like energy gap and its corresponding change in the optical properties, they are considered as the front runners in the technologically important materials. Zinc oxide (ZnO) is attracting tremendous attention due to its interesting properties like a wide direct band gap of 3.4 eV at room temperature and high exciton binding energy of 60 meV. Zinc oxide is low cost and non – toxic in nature so environmentally friendly as compared to other metal oxides (1). Band gap of ZnO material can be adjusted by appropriate doping material (eg. Mn,Al,Ni,Fe,La,Ce and Cd, etc) (2).

The detailed study of the structural, morphological and optical properties rare earth element (REE) doped ZnO nanoparticles are technologically important, as they have potential applications for flat panel displays due to enhanced emission in the visible range (3-5). Even though some of the research works have been carried out on La-doped ZnO (6 -13). The detailed study of the structural, morphological and optical properties of La and Cu co-doped ZnO_2 nanopowder is still scanty. Therefore, in the present

investigation, the major objective is to prepare La-doped and La, Cu co-doped ZnO_2 nanoparticles by co-precipitation method. The effects of Cu substitution on its structural and optical properties have been studied extensively.

Many physical and chemical methods have been developed to obtain these starting nanoparticles. They are, the solid state reaction (14), chemical vapor transport (CVT) (15), mechanochemical processing (16), sol–gel/ Co-precipitation method (17) among these different methods, co-precipitation method is one of the most important techniques to prepare nanoparticles.

2. Materials and experimental procedure

2.1. **Synthesize of $Zn_{0.96-x}La_{0.04}Cu_xO$ (x = 0, 0.02 & 0.04) nanoparticles**

$Zn_{0.96-x}La_{0.04}Cu_xO$ (x = 0, 0.02 & 0.04) nanoparticles were prepared by chemical co-precipitation method. For the synthesis of $Zn_{0.96-x}La_{0.04}Cu_xO$ sample, Zinc chloride pentahydrate ($ZnCl_4.5H_2O$), lanthanum chloride heptahydrate ($LaCl_3.7H_2O$), copper chloride dehydrate ($CuCl_2.2H_2O$) and sodium hydroxide (NaOH) were used as precursors without further purification. All the used chemicals are highly pure and AR grade from Merck. The appropriate amount of $ZnCl_45H_2O$, $LaCl_3.7H_2O$, and $CuCl_2.2H_2O$ were dissolved in 50 ml double distilled water and kept stirring until getting a clear solution. NaOH solution was prepared separately by dissolving an appropriate amount of NaOH in 50 ml double distilled water. The prepared NaOH solution was added dropwise to the initial solution to increase the pH to 9. To ensure the completion of reactions, the system was stirred continuously for 3 hrs at room temperature. The precipitations were filtered and then washed several times using double distilled water to eliminate the impurities and chlorine ions from precipitates. The collected precipitates were dried in an oven at $100°C$ for 1 hr. Finally, the synthesized powders were annealed at $500°C$ in the air atmosphere for 4 hrs followed by furnace cooling. The same procedure is repeated for the remaining samples synthesized with nominal compositions of $Zn_{0.96-x}La_{0.04}Cu_xO$ (x= 0, 0.02 &0.04) nanoparticles.

2.2 Characterization Techniques.

The crystal structure of $Zn_{0.96-x}La_{0.04}Cu_xO$ (x= 0, 0.02 &0.04) nanoparticles were determined by powder X-ray diffraction. XRD pattern was recorded by RigaKu C/max-2500 diffractometer using Cu Kα radiation (λ = 1.5408 Å) operated at 40 kV and 100 mA from 30° to 70°. The surface morphology was studied using a scanning electron microscope (SEM, Philip XL 30). The topological features and the composition of Zn, La, Cu, and O were determined by energy-dispersive X-ray spectrometer on K and L lines. A Silicon drift detector was used as a detector. The detector is cooled using a reservoir of liquid nitrogen. The vacuum is maintained at a low energy level to prevent the condensation of molecules on the crystal. The accuracy (sensitivity) of this technique is ± 1% (0.01).

The UV-Visible optical absorption and transmittance spectra of $Zn_{0.96-x}La_{0.04}Cu_xO$ (x= 0, 0.02 &0.04) nanoparticles have been carried out to exploring their optical properties. The spectral absorption spectra were recorded using a UV visible spectrophotometer (Model: Lambda 35, Make: Perkin Elmer) in the wavelength ranges from 300 to 600 nm using cm^{-1} quartz cuvettes at room temperature. Halogen and deuterium lamps were used as

sources for visible and UV radiations, respectively at room temperature. The presence of chemical bonding in $Zn_{0.96-x}La_{0.04}Cu_xO$ (x= 0,0.02 &0.04)   nanoclusters was studied by FTIR spectrometer (Model: PerkinElmer, Make: Spectrum RX I) in the range of 400 to 3900 cm^{-1}.

3. Results and discussion

3.1. X-ray diffraction (XRD) – structural studies

The XRD pattern of $Zn_{0.96-x}La_{0.04}Cu_xO$ (x = 0 ,0.02 &0.04) nanoparticles were recorded in the diffraction angle 30 to 70 are shown in Fig. 1.
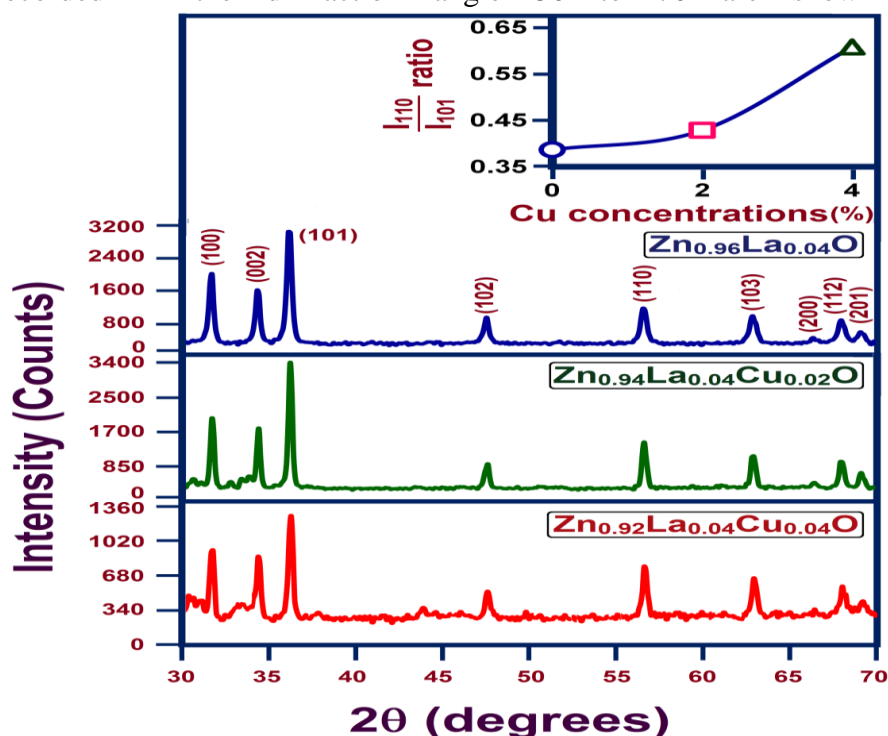

Fig 1. X-ray diffraction pattern of $Zn_{0.96-x}La_{0.04}Cu_xO_2$ nanoparticles with different Cu concentrations from 0% to 4% at room temperature.

The diffraction peaks of $Zn_{0.96-x}La_{0.04}Cu_xO$ (x= 0 ,0.02 &0.04) nanoparticles clearly shows the crystalline nature corresponding to the diffraction angles XRD pattern shows the close agreement with the standard JCPDS file for ZnO (JCPDS 36-1451, lattice constants a = b = 3.2488 nm and c = 5.2061 nm). The peaks are quite sharper indicating the crystalline nature of the prepared samples. No other characterization peaks are corresponding to oxides of Zn/ Cu/La or Cu/La related secondary and impurity phases were observed which confirmed that the product obtained in pure phase.
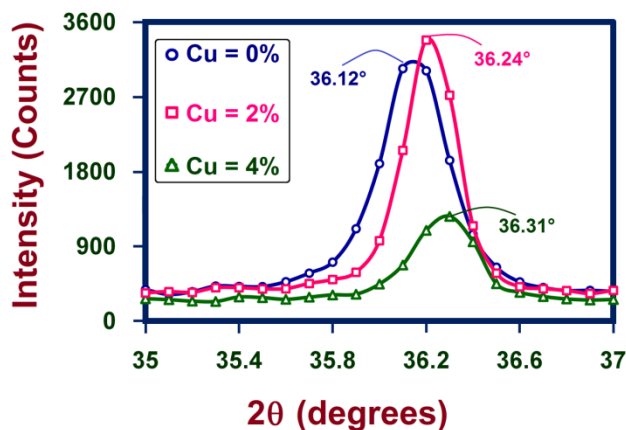
Fig.2. The enlarged image of the diffraction peak corresponding to (101) plane
        of $Zn_{0.96-x}La_{0.04}Cu_xO_2$ (x = 0, 0.02& 0.04) nanoparticles

The enlarged image of the diffraction peak corresponding to (101) plane of $Zn_{0.96-x}La_{0.04}Cu_xO_2$ nanoparticles between 35° and 37° is shown in Fig. 2 which is used to study the Cu doping effect on peak position and peak intensity. The peak intensity is increased and the peak position is shifted towards a higher 2θ side when 2% of Cu is introduced into the Zn-La-CuO lattice. Further increase of Cu-doping concentration, beyond 2%, the peak position is shifted towards the lower 2θ.   The average crystal size of the nanoparticles is calculated after appropriate background correction from X-ray line broadening of the diffraction peaks of (101) plane using Debye Scherrer's formula (18),

Average crystal size D= 0.9λ / βcosθ   (3.1)

Where λ is the wavelength of X-ray used (1.5406 Å), β is the angular peak width at half maximum in radian along (101) plane and θ is Bragg's diffraction angle.
        The c/a ratio has also been found to show a good match with ideally close-packed hexagonal structure. The volume of the unit cell for the hexagonal system has been calculated from the following equation (19)

Volume (V) = 0.866 x a^2 x c   (3.2)

Sample	Peak position	FWHM	d	D	A	C	c/a	V
$Zn_{0.96}La_{0.04}O_2$	36.1175	0.3512	2.4849	23.392	3.2578	5.2244	1.603	48.017
$Zn_{0.94}La_{0.04}Cu_{0.02}O_2$	36.2437	0.3341	2.47654	25.018	3.2461	5.2105	1.605	47.548
$Zn_{0.92}La_{0.04}Cu_{0.04}O_2$	36.1889	0.2942	2.48016	28.406	3.2515	5.2161	1.604	47.933

Table 1 shows the variation of peak position (2θ), FWHM value, d-value, unit cell parameters 'a' and 'c', c/a ratio, average crystallize (D) and Volume (V) of $Zn_{0.96-x}La_{0.04}Cu_xO_2$ nanoparticles with different Cu concentrations from 0% to 4%.

It is noticed from that even though the d-value and the lattice constant are affected by Cu-doping in Zn-La-CuO$_2$ lattice, the resultant compound maintains a hexagonal structure. When adding Cu concentration, the average crystal size is increased from 23.92 nm (Cu = 0%), 25.018 nm (Cu = 2%) and 28.406 (Cu =4%) . The increment in average crystal size is due to the smaller ionic radii of Zn^{2+} (0.69 Å) ion than dopant Cu^{2+} (0.73 Å) ion (20).

The doping of Cu (2% and 4%) decreases the micro strain from 1.4818 (Cu = 0%) to 1.3855 (Cu=2%) and 1.2202 (Cu=4%).The change in micro strain supports the crystal size. The micro-strain (ε) can be calculated using the formula (21),

Micro-strain $\varepsilon= \beta \cos\theta / 4$ $\qquad\qquad\qquad\qquad\qquad\qquad$ (3.3)

The Zn–O bond length has been calculated using the relationship (22)

Bond length (l) = $\qquad\qquad\qquad\qquad\qquad\qquad\qquad\qquad$ (3.4)

$$\sqrt{\left(\frac{a^2}{3} + \left(\frac{1}{2}-u\right)^2 c^2\right)}$$

where, $u = \frac{a^2}{3c^2} + 0.25$ is the potential parameter of the hexagonal structure.

The stress (σ) in the ZnO planes can be calculated using the following expression (23),

$\qquad\qquad \sigma = -233\times10^9 \ ((C_{bulk} - C)/ C_{bulk})$ $\qquad\qquad\qquad\qquad$ (3.5)

where, C is the lattice constant of ZnO planes calculated from XRD data, C_{bulk} is the strain-free lattice parameter of ZnO (5.2061 Å). All the samples had a negative stress, as are shown in Table 2

Sample	Bond length(l)	Micro strain(ε)	Stress σ
$Zn_{0.96}La_{0.04}O_2$	1.9833	1.4818	0.819
$Zn_{0.94}La_{0.04}Cu_{0.02}O_2$	1.9767	1.3855	0.2004
$Zn_{0.92}La_{0.04}Cu_{0.04}O_2$	1.9873	1.2202	0.4502

Table 2 shows the Bond length, Micro strain and stress value for $Zn_{0.96-x}La_{0.04}Cu_xO_2$ nanoparticles with Cu concentrations from 0% to 4%.

3.2. Microstructure and composition

The surface morphological studies of La-doped and La, Cu co-doped $ZnO2$ nanopowders were carried out using SEM images. Fig. 3 illustrates the surface morphology of $Zn_{0.96-x}La_{0.04}Cu_xO_2$ nanoparticles with different Cu concentrations from 0% to 4%. These images reveal that the crystalline nature and uniformity of each sample consists of large aggregates.
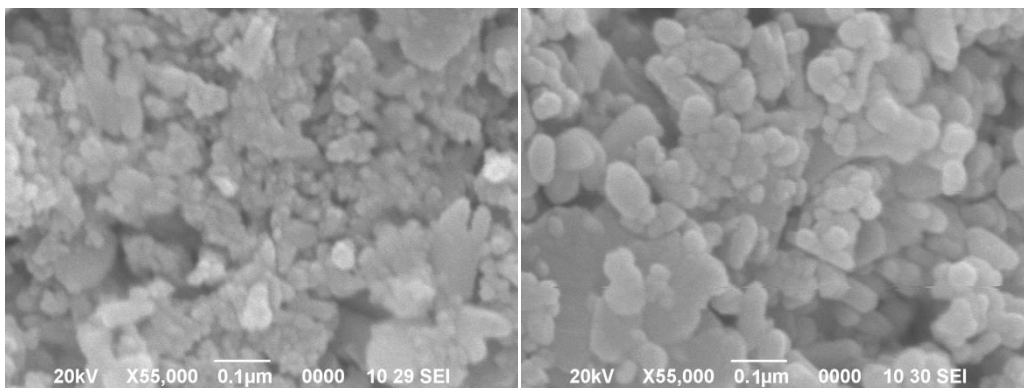
Fig (3a) shows the SEM image for $Zn_{0.96}$-$La_{0.04}O_2$ nanoparticles

Fig (3b) shows the image for $Zn_{0.94}La_{0.04}Cu_{0.02}O_2$ nanoparticles
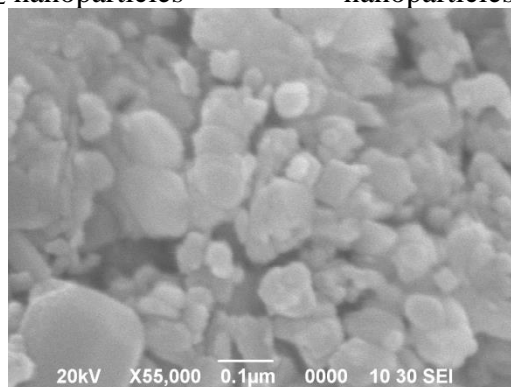
Fig (3c) shows the SEM image for $Zn_{0.92}La_{0.04}Cu_{0.04}O_2$ nanoparticles

Elements	Atomic%
O	43.23
Zn	54.60
La	2.17
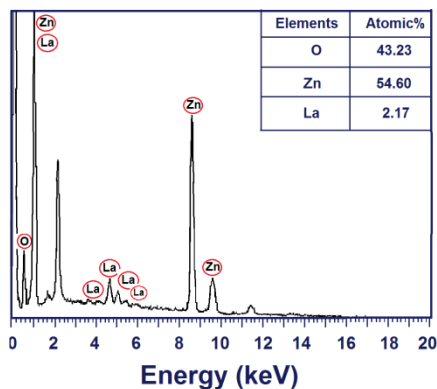
Fig. (4a) shows the EDX analysis for $Zn_{0.96}La_{0.04}O_2$ nanoparticles.

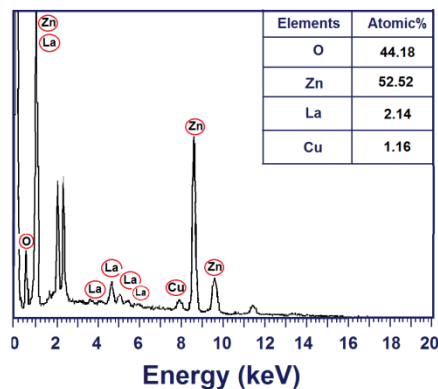| Elements	Atomic%
O	44.18
Zn	52.52
La	2.14
Cu	1.16

Fig. (4b) shows the EDX analysis for $Zn_{0.94}La_{0.04}Cu_{0.02}O_2$ nanoparticles.
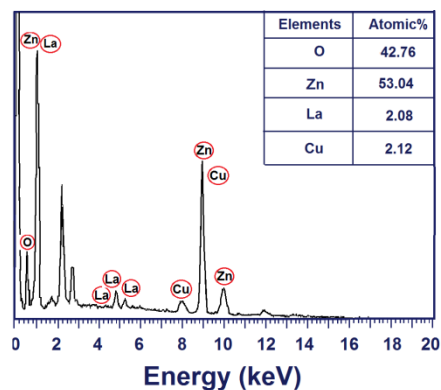
Fig.(4c) shows the EDX analysis for $Zn_{0.92}La_{0.04}Cu_{0.04}O_2$ nanoparticles.

It is observed from Fig. 4 that the presence of O is decreased (Cu=4%) but the existence of Zn is decreased by Cu-doping in $Zn_{0.96}La_{0.04}O_2$. It clearly shows that the oxygen deficiency is gradually increased in addition to Zn rich phase by Cu-doping which supports the existence of Zn interstitials at higher Cu concentrations. The EDX spectra show that the atomic% is nearly equal to their nominal stoichiometry within the experimental error.
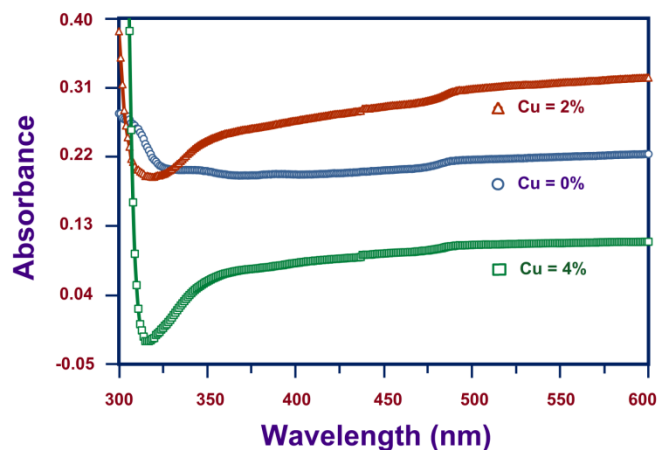
3.3. Optical studies

Fig. 5 UV–Visible absorption spectra of $Zn_{0.96-x}La_{0.04}Cu_xO_2$ nanoparticles for different Cu concentrations from 0% to 4% between 300 and 600 nm at room temperature.

Fig. 5 express the optical absorption spectra of La-doped and La, Cu co-doped ZnO_2 nanoparticles from 300 to 600 nm. The absorbance is expected to depend on several factors, such as bandgap, oxygen deficiency surface roughness, and impurity centers. La-doped and La, Cu co-doped ZnO_2 nanoparticles has low absorbance in the ultraviolet region (lower wavelength) of the spectrum and a strong absorbance in the visible region (higher wavelength). The absorbance spectra show an ultraviolet cut-off around 320 nm, which can be attributed to the photo-excitation of electrons from the valence band to the conduction band. The intensity of absorption increases abruptly as the concentration of Cu increases to 2% but it starts to decreases with further increase of Cu doping. The increasing absorption by initial doping of Cu may be the density of the defects and hence the intensity of optical absorption $Zn_{0.94}La_{0.04}Cu_{0.02}O_2$ nanoparticles. The further increase of Cu after

2% should lead to the reduction of absorption may be due to the removal of defects and disorderness present in the sample.
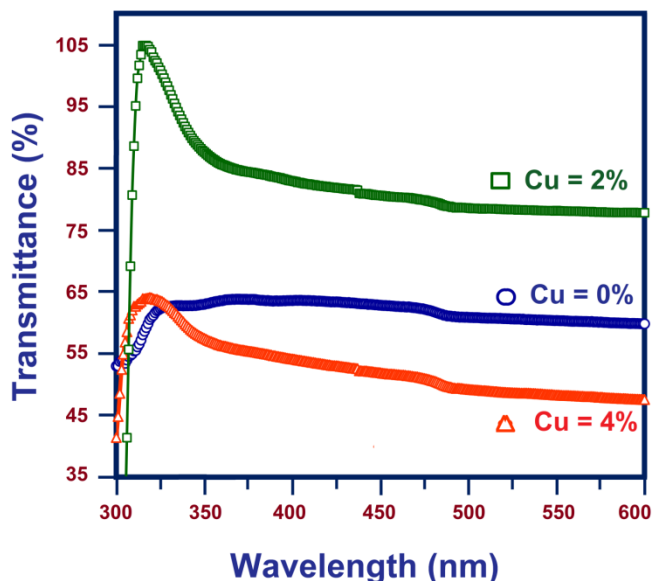

Fig 6. Transmittance spectra of $Zn_{0.96-x}La_{0.04}Cu_xO_2$ nanoparticles for different Cu
　　　Concentrations 　from 0% to 4% between 300 and 600 nm at room temperature,

Fig. 6 shows the transmittance spectra of La-doped and La, Cu co-doped ZnO_2 nanoparticles at room temperature from 300 to 600 nm. The initial doping of Cu (Cu = 2%) increases the transmittance and shows the highest transmittance about 95% and above. The transmittance values are decreased for the next higher levels of doping after Cu = 4%. This suggests that the decrease in the transmittance of Cu doped $Zn_{0.96}La_{0.04}O_2$ nanoparticles with increasing in doping concentration may lead to an increase in the degenerate (metallic) nature, which results in the increased absorption. The best optical transparency and lower absorption observed at $Zn_{0.94}La_{0.04}Cu_{0.02}O_2$ nanoparticles seem to be optimal for industrial applications, especially as the transparent electrode. The optical band gap is evaluated using the Tauc relation (24):

$$\alpha h\gamma = (Ah\gamma - Eg)^n \tag{3.6}$$

where A is a constant, Eg is the optical bandgap of the material and the exponent n depends upon the direct/indirect allowed transition. In the present case, n is taken as ½ because of allowed direct transition.
The Tauc plot is used to calculate the band gap of $Zn_{0.94-x}La_{0.04}Cu_xO_2$ nanoparticles shown in Fig. 7.
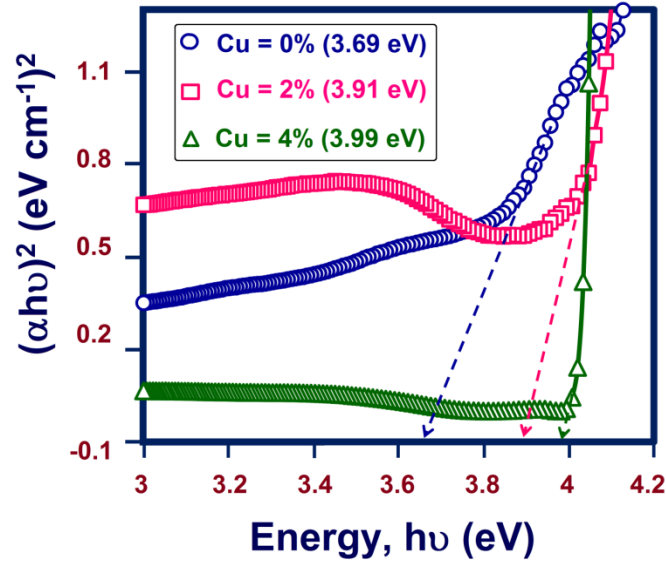
Fig.7. Shows the energy band gap values for $Zn_{0.96-x}La_{0.04}Cu_xO_2$ nanoparticles for different Cu concentrations from 0% to 4%.

The energy gap of $Zn_{0.96}La_{0.04}$ O nanoparticles is 3.69 eV . The doping of Cu sharply increases the energy gap from 3.69 eV (Cu = 0%) to 3.91 eV (Cu=2%) and 3.99 eV (Cu = 4%) (ΔEg= 0.30 eV). When Cu is introduced into Zn-La-O lattice, additional charge carriers are produced. The blue shift of Eg from Cu=0 to 4% is explained in terms of the distortion of host lattice and generation of defects.

3.4. Fourier transform infrared (FTIR) spectroscopy

 FTIR is a technique used to obtain the information about the chemical bonding in a material.
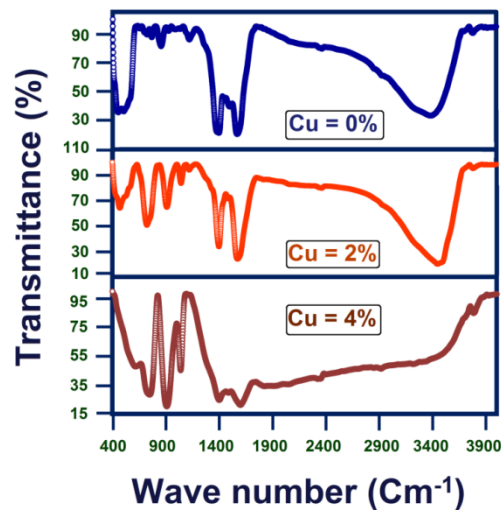

Fig. 8 shows the FTIR analysis for $Zn_{0.96-x}La_{0.04}Cu_xO_2$ nanoparticles for different Cu concentrations from 0% to 4% between 400 and 3900 nm,

From these spectra, the absorption peak around 3400 cm^{-1} is attributed to the vibration of the hydroxyl group because of the fact that the ZnO_2 retained certain adsorbed water from the ambient atmosphere (25). The weak peak at 2900 cm^{-1} belongs to the stretching vibrations of COH bonds. The O-H bending bands appearing around 1600 cm^{-1} are associated with the water molecules that exist in the nanoparticles (26) . The absorption peaks around 1300 cm^{-1} are due to the stretching vibration of the carboxyl group (C=O) (27). The characteristics below 800-900 cm^{-1} show the presence or absence of Zn-O/Cu-O/La-O bonds and their functional groups. The vibration of anti-symmetric O-Zn-O bridge functional groups is related to the wavenumbers between 400 and 600 cm^{-1} and the absorption between 600 and 800 cm^{-1} is corresponding to a lattice mode of ZnO_2 (28).

4. Conclusion

La-doped and La, Cu co-doped ZnO_2 nanoparticles have been synthesized by the co-precipitation method. The structural and optical properties of the synthesized nanoparticles were analyzed using X-ray diffraction, UV–visible spectra, and Fourier transforms infrared techniques. From XRD measurements, it was confirmed that the particle size of the synthesized $Zn_{0.94-x}La_{0.04}Cu_xO_2$ decreases with increasing copper concentrations and possess hexagonal wurtzite structure. The variation in size and shape of the grains in the $Zn_{0.96}La_{0.04}O_2$ lattice by Cu-doping was discussed using a scanning electron microscope. FTIR spectra of $Zn_{0.96-x}La_{0.04}Cu_xO_2$ nanoparticles for different Cu concentrations from 0% to 4% at room temperature. The elemental compositions were confirmed by EDX analysis. The energy gap from 3.69 eV (Cu = 0%) to 3.99 eV (Cu = 4%) (ΔEg = 0.30 eV) is due to the distortion in the crystal structure. The best optical transparency observed at $Zn_{0.94}La_{0.04}Cu_{0.02}O_2$ nanoparticles seems to be optimal for industrial applications.

References .

1. G.Kaur,A.Mitra,K.I.Yadav,Growth and properties of pulsed laser deposited Al-doped ZnO thin film.Adv.Mater.Letr.6(1)(2015) 73-79.
2. R.A.Zargar,S.Chackrabarti,Md.Shahabuddin,J.Kumar,A.K.Hafiz,Novel composites of Zn1-xCdxO (x=0,0.5,0.1) thick films for optoelectronic device applications.J.Mater.Sci.Mater .Electron.26(2015)10027-10033.
3. T. Tsuzuki, P.G. McCormick, Scr. Mater. 44 (2001) 1731.
4. W.E. Mahmoud, J. Crystal Growth 312 (2010) 3075.
5. W. Gao, Z.W. Li, J. Alloys Compd. 449 (2008) 202.ZnNdCu
6. M. Ungureanu, H. Schmidt, Q. Xu, H. von Wenckstern, D. Spemann, H. Hochmuth, Superlattices Microstruct. 42 (2007) 231.
7. R.Govindaraj,R.Govindan,M.Geetha,P.Anbarasan,Structural , morphological qand luminescence studies of pristine and La doped Zinc Oxide (ZnO) Sinter,45 (2013)13-19
8. Preeti Chaudhary,Priti Singh,Vipin Kumar,Synthesis and Characterization of pure ZnO and La doped ZnO (Zn 0.98La0.020) films via novel sol-gel screen printing method , Elsevier volume 158, April 2018 pages 376-381

9. V.Porkalai,D.Benny Anburaj , B.Sathya, C.Nedunchezhian,R.Meenambika (2017) study the synthesisstructural optical and electrical properties of ZnO and Lanthanum doped ZnO nanoparticles by sol-gel method ,Mechanics Meterials science &Engineering , Vol 9DOI 10.2412/mmse.77.37.393.

10. S.Prabhavathy & R.Jothilakshmi "Preparation and characterization of pure and lanthanum doped ZnO nanoparticles by solution route" Materials Science Forum,Vol 807.PP 123-133,2015

11. Rare Earth Element (REE) lanthanum doped zinc oxide (La: ZnO) nanomaterials . Synthesis structural optical and antibacterial studies. Journal of Alloys and Compounds , 723 PP 1155-1161.ISSN 1873-4669.

12. Mohamed Shabon, A.M.Fi Sayed, Effects of lanthanum and sodium on the structural optical and hydrophilic properties of sol-gel derived ZnO films ,A Comparative study. Elsevier Materials Science in semiconductor processing vol 41, Jan 2016 pages 323-334.

13. M.H.tang,Z.Q.Zeng,J.C.Li,Z.P.Wang,X.L.Xu,G.Y.Wang,L.B.Zhang,S.B.Yang,Y.G .Xiao,B.Jiang,Resistive switching behavior of La-doped ZnO films for non volatile memory application.Elsevier Solid state electronics vol 63,issue 1, sep 2011 pages 100-104.

14. C.C. Hwang, T.W. Wu, J. Mater. Sci. 39 (2004) 6111.

15. C.F. Jin, X. Yuan, W.W. Ge, J.M. Hong, X.Q. Xin, Nanotechnology 14(6) (2003) 667.

16. Z.X.Cheng,X.L.Wang,S.X.Dou,K.Ozawa,H.Kimura,P.Munroe,J.Phys.D.Appl.Phys. 40(21)(2007) 6518.

17. H. Udono, Y. Sumi, S. Yamada, I. Kikuma, J. Cryst. Growth 310 (2008) 1827.

18. Y.Bouznit[a]Y.Beggah[a]F.Ynineb[b] Sprayed lanthanum doped zinc oxide thin films, Applied Surface Science, Volume 258, Issue 7, 15 January 2012, Pages 2967-2971

19. P. P. Hankare, P A. Chate, D. J. Sathe, P. A. Chavan, V. M. Bhuse, J. Mater. Sci: Mater. Electron. 20 (2009) 374.

20. G.Srinivasan,R.T.R.Kumar,J.Kumar,J.Sol-Gel Sci.Technol.43(2007) 171-177.

21. S. Muthukumaran, R. Gopalakrishnan, Physica B 407 (2012) 3448.

22. M.S.Kim,J.B.Yang,Q.Cai,X.D.Zhou,W.J.James,W.B.Yelon,P.E.Parris,D.Buddikot, S.K.Malik,J.Appl.Phys.97 (2005)10H714.

23. B.D. Cullity, Elements of X-ray Diffractions, Addison-Wesley, Reading, MA, 1978.

24. S. Anandan, S. Muthukumaran, M. Ashokkumar, Superlattices and Microstructures 74 (2014) 247.

25. E. Burstein, Phys. Rev. 93 (1954) 632.

26. M. Arshad, A. Azam, A.S. Ahmea, S. Mollah, A.H. Naqvi, J. Alloys Compd. 509 (2011) 8378. 38.X.Y. Li, H.J. Lia, M. Yuan, Z.J. Wang, Z.Y. Zhou, R.B. Xu, J. Alloys Compd. 509 (2011) 3025.

27. X.Y. Li, H.J. Lia, M. Yuan, Z.J. Wang, Z.Y. Zhou, R.B. Xu, J. Alloys Compd. 509 (2011) 3025.

28. S. Senthilkumar, K. Rajendran, S. Banerjee, T.K. Chini, V. Sengodan, Mater. Sci. Semi. Process 11 (2008) 6.

<u>Authors</u>

First author: D.ANBUSELVAN, M.Sc.,M.Phil.,B.Ed,
         P.G. and Research Department of Physics,

         Rajah Serfoji Government College(Autonomous), Thanjavur-5

         (Affiliated to Bharathidasan university)

Second Author: S.ANANDAN.M.Sc.,M.Phil.,Ph.D.,

         P.G.and Research,Department of Physics,

         Thiru.Vi.Ka.Govt Arts College Thiruvarur-3

         (Affiliated to Bharathidasan university)

Third author & Corresponding author :
         S.NILAVAZHZGAN M.Sc.,M.Phil.,Ph.D.,B.Ed.,PGDCA.,
         P.G. and Research Department of Physics

         Rajah Serfoji Government College(Autonomous), Thanjavur-5

         (Affiliated to Bharathidasan university)

         Email ID:snila1977@gmail.com.

         Contact no:9443586433